[10]F. O. Ellison and Ay-Ju A. Wu, J. Chem. Phys. **47**, 4408 (1967).
[11]R. L. Champion, L. D. Doverspike, W. G. Rich, and S. M. Bobbio, Phys. Rev. A 2, 2327 (1970).
[12]R. L. Champion, L. D. Doverspike, and T. L. Bailey, J. Chem. Phys. **45**, 4377 (1966).
[13]N. F. Mott and H. S. W. Massey, *The Theory of Atomic Collisions* (Oxford U.P., London, 1965).
[14]F. B. Hildebrand, *Introduction to Numerical Analysis* (McGraw-Hill, New York, 1956).

PHYSICAL REVIEW A VOLUME 7, NUMBER 5 MAY 1973

Study of the L- and M-Shell X Rays of Pb Produced by 0.5 – 14.0-MeV-Proton Beams*

C. E. Busch, A. B. Baskin, P. H. Nettles,† and S. M. Shafroth
University of North Carolina at Chapel Hill, Chapel Hill, North Carolina 27514
Triangle Universities Nuclear Laboratories, Durham, North Carolina 27706

A. W. Waltner
North Carolina State University, Raleigh, North Carolina 27607
Triangle Universities Nuclear Laboratories, Durham, North Carolina 27706

(Received 31 October 1972)

The L and M x rays of Pb were observed with a Si(Li) detector of 190-eV resolution for a 6-keV x-ray line. Absolute shell-ionization cross sections were derived and compared to plane-wave-Born-approximation (PWBA) and binary-encounter-approximation (BEA) predictions. The agreement between theory and experiment was generally good for both cross sections and x-ray ratio predictions. For proton energies less than 3 MeV the $L\alpha/L\beta$ and $L\alpha/L\gamma$ ratios display deviations that are qualitatively predicted by both theories but only absolutely reproduced by the PWBA result for $L\alpha/L\beta$. The $L\alpha/Ll$ ratio exhibits a minimum in the proton energy range 0.5–3.0 MeV that is not predicted by a single-ionization-state process.

I. INTRODUCTION

Growing interest in characteristic x-ray production by proton bombardment has resulted recently in measurements involving the K, L, and M shells.[1–4] Measurements of x-ray production are usually compared with predictions of theoretical models of the ionization process described by the plane-wave Born approximation (PWBA),[5] the binary-encounter approximation (BEA),[6] or the semiclassical approximation (SCA).[7] The agreement between theory and experiment is generally good in the K- and L-shell-ionization cross sections for proton energies considerably larger than the electron binding energies involved, and at lower proton energies for higher-Z targets.[1,8] Discrepancies for various L-shell x-ray ratio predictions have been observed, however, for protons on Au.[8] The primary difficulty in comparing observed x-ray yields with theoretical predictions is the fluorescence-yield correction including radiationless (Auger) and Coster-Kronig (CK) transitions. For K-shell ionization the fluorescence yield is accurately established for most of the heavy elements. This is not the case for the L and M shells, where a knowledge of the subshell fluorescence yields and Coster-Kronig transition probabilities is required, but available in only a few cases for the L shell and not at all for the M shell.

This work presents the results of a study of L and M x-ray production by incident protons in the energy range 0.5–14.0 MeV on lead targets. The observed L and M absolute x-ray production and relative yields for the L x-ray components were measured as a function of incident proton energy and compared to available theoretical predictions.

II. EXPERIMENT

A. Apparatus

The general experimental arrangement has been previously described[1] and only details related to measurements made with lead targets will be discussed. A proton beam from the TUNL-FN-tandem–Van de Graaff accelerator was used for the 2–14-MeV measurements and the TUNL-4-MeV Van de Graaff accelerator covered the 0.5–3.0-MeV range.

A cubic aluminum target chamber, aluminum target rod, and graphite target ring similar in design to those previously mentioned were employed to reduce background contributions to the observed spectrum in the photon energy range of interest. The liquid-nitrogen-cooled Si(Li) detector, located at a scattering angle of 90° with respect to the incident beam, had a resolution of 190 eV for the Cu$K\alpha$ line and an effective area of 30.0 mm^2. The detector was constructed with a 0.001-in.-thick Be

window, which greatly facilitated the measurements of low-energy L and M x rays. The detection efficiency of the detector for the observed photon energies was obtained by a direct comparison of counting rates obtained under identical conditions for this detector and a similar Si(Li) detector previously calibrated.[1] It was found that the detection efficiency for all Pb L x rays was 1.00 ± 0.01 and 0.36 ± 0.10 for the Pb M x rays.

The data were normalized to the charge integrated from the beam collected in the Faraday cup after passage through the target foil. The data taking was terminated for each run by a preset scaler driven by the output signal from the current integrator. The scaler was gated by a signal derived from the computer dead time and thus provided an automatic dead-time correction. This dead-time correction was found to be accurate to 1.0% by using a precision 60-Hz pulser to simultaneously insert a peak in the spectrum and drive a scaler gated by the computer dead time. The calibrated pulser peak also served as an energy calibration point in the spectrum. Additional energy calibration was provided by collecting the spectra of ^{55}Fe and ^{109}Cd sources.

B. 0.5-3.0-MeV Data Specifics

The detector was inserted into the beam vacuum system through one of the lateral ports of the cubic target chamber. An iron mask 0.125-in. thick and having a central hole of 0.070-in. diam was positioned over the detector surface to limit the solid angle exposed to the target to 0.0040 ± 0.0004 sr. Particular advantage was derived from placing the detector in the vacuum, since this eliminated the need for target to detector attenuation factors and their associated uncertainties.

The Pb target was prepared by evaporation onto a 20-$\mu g/cm^2$ C foil and supported on a 0.0675-in.-thick graphite annulus having 0.5-in. i.d. and 0.75-in. o.d. The Pb target thickness was determined to be 34.7 ± 3.5 $\mu g/cm^2$ by observing the Rutherford scattering of the incident protons at 2.0 and 1.75 MeV in the x-ray detector. This method has the advantage of measuring the effective target thickness for the identical geometry used in the x-ray measurements.

C. 2.04-14.0-MeV Data Specifics

For the data obtained with the FN Tandem Accelerator, the detector was separated from the vacuum by a 0.001-in. Mylar window over the lateral port and an air gap of 12.5 mm. A lucite annular mask 2.0 mm thick with 1.6-mm i.d. was centered over the detector to attenuate the prolific M peak and provide acceptable counting rates. The attenuation factor due to the lucite mask was measured directly for each x ray of interest in two consecutive runs—one with the mask, and one without.

The target thickness was determined as above for incident proton energies of 3.0, 4.0, and 5.0 MeV to be 700 ± 110 $\mu g/cm^2$.

D. Analysis

The observed x-ray intensities were extracted from the spectrum by a least-squares-fitting program (GAUSSN) capable of fitting up to 4 Gaussian shapes with a linear background. A sample spectrum for protons on Pb is presented in Fig. 1.

The detector resolution was sufficient to resolve only $L\alpha$, $L\beta$, $L\gamma$, Ll, $L\eta$, and M. $L\gamma$ was fitted with three Gaussians to reproduce the observed shape: However, each Gaussian is still a composite of several unresolved lines; thus the sum of the three fitted areas was used to form $L\gamma$. Similarly, the M peak is composed of a major peak of unresolved lines having an average photon energy of 2.4 keV and a tail peaking at about 3.1 keV, which were summed to produce $\sigma_{M\text{ x ray}}$.

The methods and formulas required to determine total x-ray cross sections and x-ray ratios and their comparison to theory have been discussed previously.[1,8] Briefly, the observed x-ray yield intensities $L\alpha$, $L\beta$, $L\gamma$, Ll, and M were converted to x-ray cross sections by the formula

$$\sigma_{\alpha,\beta,\gamma,l,M} = 4\pi Y_{\alpha,\beta,\gamma,l,M} / A_{\alpha,\beta,\gamma,l,M} E_{\alpha,\beta,\gamma,l,M} \phi t \Delta\Omega \ ,$$

where the angular distribution of each x ray is assumed isotropic, $A_{\alpha,\beta,\gamma,l,M}$ is the total x-ray absorption correction in the target, Mylar window, air path, and mask, $E_{\alpha,\beta,\gamma,l,M}$ is the detection efficiency for each x ray, ϕ is the number of incident protons on the target, t is the target thickness and $\Delta\Omega$ is the detector solid angle. The total L x-ray cross section is then

$$\sigma_{L\text{ x ray}} = \sigma_\alpha + \sigma_\beta + \sigma_\gamma + \sigma_l \ .$$

It should be pointed out that the analyses of the two sets of data were carried out independently and were mutually consistent, within calculated errors. It was noted, however, that in the range of common energies 2.0–3.0 MeV a systematic discrepancy of about 13% was present between the two sets of data. Systematic trends of this nature are most often due to multiplicative factors, such as target thickness or absorption corrections. There were no correction factors for absorption, except for a small target absorption correction of $A_M = 0.97$ to the M yield, in the low-energy data, whereas the attenuation factors for the Tandem data ranged from $A = 0.30$ to 0.82 for the various L's and $A_M = 0.13$. In addition, the target thickness was measured to a higher accuracy. For these reasons, the high-energy data were normalized to join smoothly to the low-energy data in the overlapping region. Experi-

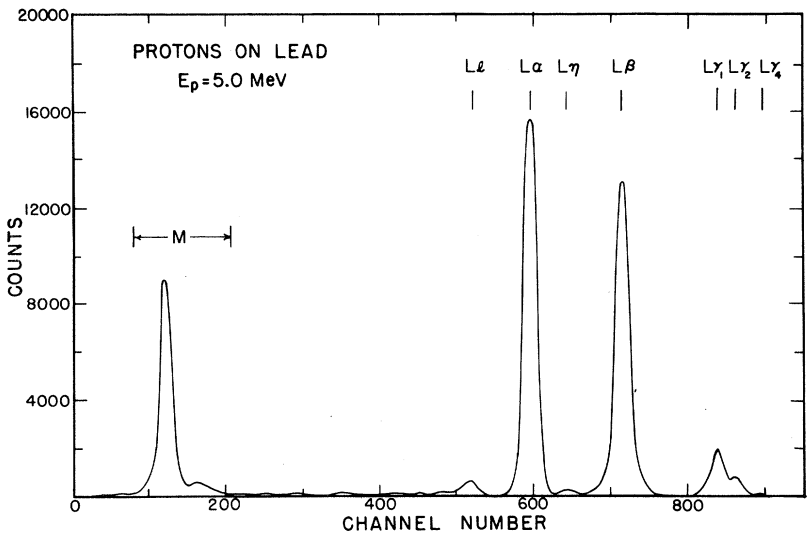

FIG. 1. Typical x-ray spectrum for 8-MeV protons incident on a lead target.

mental uncertainties for each data point include the effect of (a) counting statistics and background subtraction, (b) detection efficiency, (c) target thickness, and (d) the target to detector absorption, if present. Since the largest contributions were from target thickness and detection efficiency, the relative error from point to point is considerably smaller than indicated.

III. RESULTS AND DISCUSSION

The experimental x-ray cross sections can be compared to theoretical subshell-ionization cross sections by the use of subshell fluorescence yields and Coster–Kronig (CK) transition probabilities.[9,11] The L x-ray-production cross section is related to the subshell-ionization cross sections by the formula

$$\sigma_{L\,\mathrm{x\,ray}} = \nu_{\mathrm{I}}\,\sigma_{L_{\mathrm{I}}} + \nu_{\mathrm{II}}\sigma_{L_{\mathrm{II}}} + \nu_{\mathrm{III}}\sigma_{L_{\mathrm{III}}} \ ,$$

where the $\nu_{\mathrm{I,II,III}}$ are CK corrected subshell fluorescence yields given by

$$\nu_{\mathrm{I}} = \omega_1 + \omega_2 f_{12} + \omega_3(f_{13} + f_{12}f_{23}) \ ,$$

$$\nu_{\mathrm{II}} = \omega_2 + \omega_3 f_{23} \ , \quad \nu_{\mathrm{III}} = \omega_3 \ .$$

The ω_i's are ith subshell fluorescence yields and the f_{ij}'s are CK transition yields linking subshells i and j.

The situation is greatly complicated for the M shell, which is composed of five subshells for which no fluorescence yields are established. In this case the M x-ray production cross section $\sigma_{M\,\mathrm{x\,ray}}$ is related to the shell-ionization cross section σ_M by the average fluorescence yield $\bar{\omega}_M$ by

$$\sigma_{M\,\mathrm{x\,ray}} = \bar{\omega}_M \sigma_M \ .$$

Since $\bar{\omega}_M$ is a weighted average over the subshells and depends on the relative probability for producing a vacancy in a given subshell as well as CK transition yields, the value of $\bar{\omega}_M$ may depend on the nature of the process used in its measurement. For this reason the value of $\sigma_{M\,\mathrm{x\,ray}}$ calculated theoretically may be expected to display a systematic discrepancy from the experimental values.

The ratios $L\alpha/L\beta$, and $L\alpha/L\gamma$ are produced by folding in the theoretical subshell-ionization cross sections, the fluorescence and CK yields, and the radiative widths as described previously.[8] The ratio $L\alpha/Ll$, however, should be a constant given by

$$L\alpha/Ll = \Gamma_{3\alpha}/\Gamma_{3l} \ ,$$

where $\Gamma_{3\alpha,3l}$ is the sum of the radiative widths for transitions filling the hole in the L_{III} subshell which contribute to the $L\alpha, l$ line. This occurs since both $L\alpha$ and Ll originate from the filling of a hole in the L_{III} subshell exclusively.

The L-subshell-ionization cross sections ($\sigma_{L_{\mathrm{I}}}$, $\sigma_{L_{\mathrm{II}}}$, $\sigma_{L_{\mathrm{III}}}$), used to generate the BEA theoretical predictions in this work were scaled from K-shell cross sections according to the prescription of Garcia.[6] The M-shell-ionization cross section was similarly derived using an average binding energy for the M shell formed by weighting the subshell binding energies by the number of electrons per subshell. The PWBA L-subshell cross sections were calculated by Choi[10] using nonrelativistic atomic wave functions.

A. L and M X-Ray-Production Cross Sections

The L x-ray cross-section results are shown in Fig. 2 and are listed in Table I for incident proton energies from 0.44 to 14.0 MeV. The BEA and PWBA predictions for L x-ray are also superimposed over the data. These curves were generated from the calculated L-subshell-ionization cross sections using the values $\omega_1 = 0.07 \pm 0.02$, $\omega_2 = 0.363 \pm 0.015$, $\omega_3 = 0.315 \pm 0.013$, $f_{12} = 0.15 \pm 0.04$, f_{13}

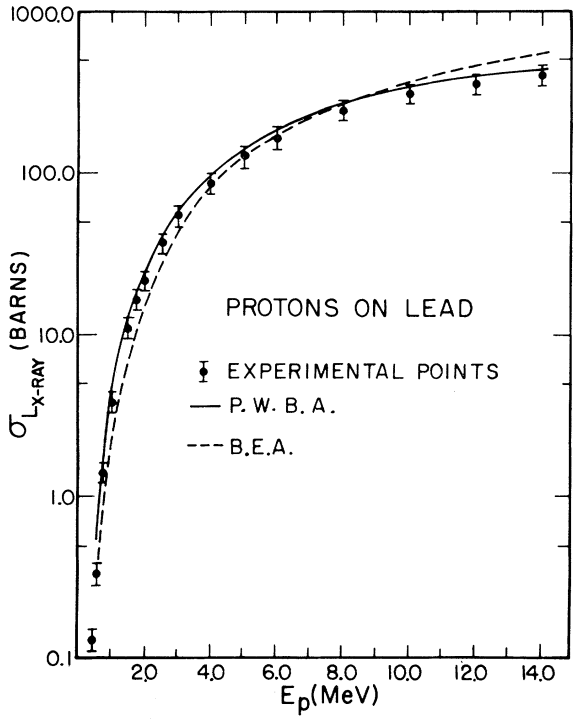

FIG. 2. L x-ray-production cross sections for incident proton energies in the range 0.5–14.0 MeV.

$= 0.57 \pm 0.03$, and $f_{23} = 0.164 \pm 0.016$ all taken from the results of Rao given by Bambynek *et al.*[11] The data do not include the effect of experimental errors contained in fluorescence yields and CK yields in the theoretical calculations of $\sigma_{L\,\mathrm{x\,ray}}$. The theoretical predictions for both theories are quite close to the experimental values over the investigated range. The BEA curve is seen to deviate from the data by about 25% for proton energies above 8 MeV and below 3 MeV, being, respectively, higher and lower than measured values. The PWBA faithfully reproduces the data over the entire energy range within experimental errors.

The experimental data and theoretical predictions for the M x-ray cross section are displayed in Fig. 3. The value for the average M-shell fluorescence yield used to convert the average theoretical M-shell-ionization cross sections to x-ray cross sections was $\bar{\omega}_M = 0.029$.[11] The BEA prediction for $\sigma_{M\,\mathrm{x\,ray}}$ is systematically about 20% lower than the data over the proton energy range. In addition, the predicted shape differs somewhat from the data in that the BEA curve exhibits a maximum at a proton energy of about 6 MeV as compared to about 7–8 MeV experimentally and also decreases more rapidly with proton energy on either side of the maximum. The systematic shift may be the result of multiplicative factors, such as errors in the absolute detector efficiency, target attenuation, or average fluorescence yield as mentioned previously. In addition, the BEA curve was scaled from K-shell-ionization cross sections assuming a weighted average for the M-shell binding energy. Considering these problems, the lack of absolute agreement for the BEA calculation is not surprising.

B. $L\alpha/L\beta$, $L\alpha/L\gamma$, $L\alpha/Ll$ Ratios

The experimental L x-ray ratios are listed in Table II and are shown in Fig. 4. Also included in the same figure are the BEA and PWBA predictions for the $L\alpha/L\beta$ and $L\alpha/L\gamma$ ratios, as well as the expected constant value of $L\alpha/Ll$. The fluorescence yields and CK yields used to generate the theory curves are those used above for $\sigma_{L\,\mathrm{x\,ray}}$ while the radiative widths for the various components of the characteristic lines were taken from Scofield.[12]

TABLE I. Pb M and L x-ray-production cross sections for proton bombardment.

Incident Energy (MeV)	$\sigma_{M\,\mathrm{x\,ray}}$ (kb)	$\sigma_{L\,\mathrm{x\,ray}}$ (b)
0.44	0.27 ± 0.07	0.13 ± 0.02
0.53	0.36 ± 0.09	0.33 ± 0.05
0.75	0.63 ± 0.16	1.37 ± 0.19
1.00	1.02 ± 0.25	3.84 ± 0.54
1.50	1.66 ± 0.41	11.20 ± 1.50
1.75	1.96 ± 0.49	16.20 ± 2.20
2.00	2.23 ± 0.56	21.90 ± 2.90
2.50	2.43 ± 0.61	36.00 ± 5.00
3.00	3.16 ± 0.79	53.70 ± 7.50
4.00	3.68 ± 0.91	86.00 ± 12.0
5.00	4.05 ± 1.01	126.00 ± 18.0
6.00	4.15 ± 1.04	164.00 ± 23.0
8.00	4.37 ± 1.10	244.00 ± 34.0
10.00	4.17 ± 1.04	308.00 ± 42.0
12.00	3.87 ± 0.97	356.00 ± 50.0
14.00	3.75 ± 0.94	403.00 ± 56.0

TABLE II. Pb L x-ray ratios for proton bombardment.

Incident Energy (MeV)	$L\alpha/L\beta$	$L\alpha/L\gamma$	$L\alpha/Ll$
0.50	2.096 ± 0.052	···	19.81 ± 0.40
0.75	2.104 ± 0.052	20.70 ± 2.0	19.03 ± 0.32
1.00	2.062 ± 0.052	19.2 ± 1.50	18.80 ± 0.32
1.25	···	···	18.48 ± 0.30
1.50	1.883 ± 0.051	15.00 ± 1.50	18.66 ± 0.30
1.75	1.947 ± 0.051	16.60 ± 1.60	19.09 ± 0.30
2.00	1.848 ± 0.051	14.50 ± 1.60[a]	19.50 ± 0.30[a]
		13.39 ± 0.67[b]	18.87 ± 0.53[b]
2.50	1.768 ± 0.050	12.30 ± 1.20	19.60 ± 0.40
3.00	1.700 ± 0.050	12.16 ± 0.61	20.00 ± 0.40
4.00	1.667 ± 0.051	11.04 ± 0.55	18.99 ± 0.53
5.00	1.622 ± 0.052	10.96 ± 0.54	19.77 ± 0.53
6.00	1.601 ± 0.052	10.78 ± 0.42	19.14 ± 0.53
8.00	1.5 ± 0.052	10.54 ± 0.40	19.19 ± 0.51
10.00	1.573 ± 0.051	10.42 ± 0.41	19.33 ± 0.52
12.00	1.566 ± 0.050	10.36 ± 0.40	19.24 ± 0.50
14.00	1.560 ± 0.050	10.47 ± 0.40	19.29 ± 0.50

[a]Indicates data taken on 4-MeV Van de Graaf.
[b]Indicates data taken on FN Tandem.

The BEA curve describes the observed $L\alpha/L\gamma$ ratios satisfactorily for proton energies above 3.0 MeV, whereas the PWBA curve appears to fall more rapidly with increasing proton energy in this range than the data. For proton energies below 3.0 MeV, the PWBA agrees well with the data for $L\alpha/L\beta$ exhibiting a maximum at about 1 MeV, while the BEA also shows a maximum, but falls about 10% below the data. Similar results are obtained for $L\alpha/L\gamma$ with the exception that both theories predict maxima that are not established in the low-energy data.

The expected lack of incident proton energy dependence for $L\alpha/Ll$ was observed in the data for energies above 3 MeV, where an average value of about 19.23 as compared to an expected value of 18.98 was found.[12] A dip in the ratio for the lower proton energies has been observed having a minimum between 1–1.5 MeV. The reason for this behavior is not yet evident. Since both $L\alpha$ and Ll originate as holes in the L_{III} subshell, the explanation must probably lie in the initial M-shell-state configuration. $L\alpha$ is a composite of transitions from the $M_V(3d_{\frac{5}{2}})$ and $M_{IV}(3d_{\frac{3}{2}})$ subshells to $L_{III}(2P_{\frac{3}{2}})$, while Ll is a pure $M_I \rightarrow L_{III}$ transition. A possible explanation is the simultaneous ejection of L_{III} and M electrons creating an initial state of multiple ionization. A velocity-matching mechanism might be suspected, except that the incident proton velocity matches the M-shell electron velocity at $E_p = 7$–8 MeV, as is indicated by the excitation curve for M_{xray}, not at this value of $E_p \sim 1.5$ MeV. The predicted peaks in the $L\alpha/L\beta$ and $L\alpha/L\beta$ and $L\alpha/L\gamma$ ratios are primarily a result of the different proton energy dependence for the various L-subshell cross sections as a result of subshell binding-energy differences. This is evident since the peaks are predicted by BEA as well as by PWBA calculations. Similar differences in the M_I-, M_{IV}-, and M_V-subshell-ionization cross sections may cause changes in the M_I/M_{IV} and M_I/M_V ionization probabilities in such a way as to produce the observed experimental dip in the $L\alpha/Ll$ ratio, if multiple ionization is the responsible process. It is unlikely that trace target impurities could cause a dip in the observed ratio.

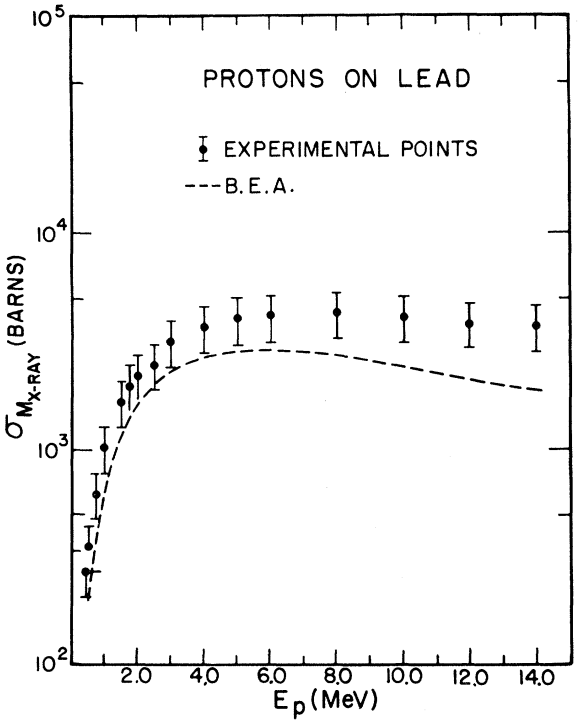

FIG. 3. M x-ray-production cross sections for incident proton energies in the range 0.5–14.0 MeV.

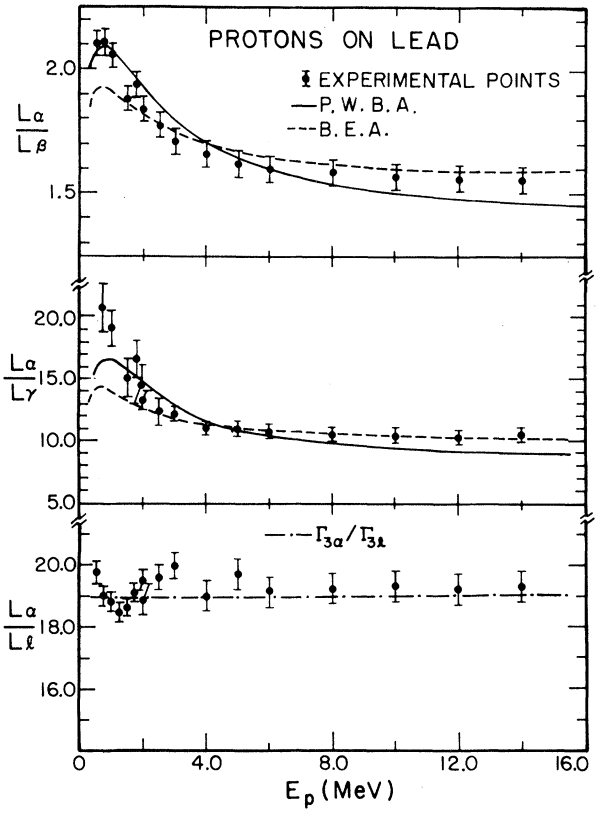

FIG. 4. $L\alpha/L\beta$, $L\alpha/L\gamma$, and $L\alpha/Ll$ x-ray ratios for incident proton energies in the range 0.5–14.0 MeV.

IV. SUMMARY

The L x-ray-production cross sections for 0.5–14-MeV protons on Pb have been measured and compared to predictions based on the BEA and PWBA theories. Both theories agree well with the data over this proton range, although the PWBA prediction reproduces the $\sigma_{L\ xray}$ shape to a better

degree than the BEA. The M x-ray-production excitation function over the same proton energies has also been compared to the BEA predictions. In this case the BEA curve shows about a 20% smaller cross section and a shape that falls from a maximum value at $E_p \approx 6.0$ MeV more rapidly than the data which has a maximum at $E_p \approx 8$ MeV.

The x-ray ratios $L\alpha/L\beta$, $L\alpha/L\gamma$ and $L\alpha/Ll$ were also observed and compared to BEA and PWBA theories. For the cases of $L\alpha/L\beta$ and $L\alpha/L\gamma$, the BEA predictions agree with the data over the proton range 3–14 MeV, but the PWBA falls more rapidly than the data with increasing proton energy. The PWBA agrees well with the data for $E_p = 0.5$–3.0 MeV for $L\alpha/L\beta$, while the BEA prediction is about 10% low. Both theories fail to reproduce the observed $L\alpha/L\gamma$ ratios for the low-energy-proton data.

The ratio $L\alpha/Ll$ displays little dependence on proton energy for values of E_p greater than 4 MeV as expected. A curious minimum is observed in the range $E_p = 0.5$–3.0 MeV; however, that has not yet been satisfactorily understood.

Further studies are indicated to look for the observed minimum in $L\alpha/Ll$ for other targets and in the same target for heavy incident particles. Improved detector resolution would allow the separation of the individual components of $L\gamma$ and $L\beta$ which may also exhibit the observed minimum. This would also allow the direct determination of the ionization cross section for each L subshell. Investigation of the M x rays with improved resolution may also yield M x-ray ratio results leading to the explanation of the dip in $L\alpha/Ll$.

ACKNOWLEDGMENTS

We are grateful to Dr. Eugen Merzbacher for his continued interest and helpful discussions during the course of this experiment. We would also like to express our gratitude to Dr. B.-H. Choi for providing the PWBA calculations used throughout this work. For their assistance in the data gathering process, we would like to thank W. Scates and B. Doyle.

†Present address: Scientific-Atlanta, Box 13654, Atlanta, Ga.

*Work supported by U. S. Atomic Energy Commission.

[1]G. A. Bissinger, J. M. Joyce, E. J. Ludwig, W. S. McEver, and S. M. Shafroth, Phys. Rev. A **1**, 841 (1970); G. A. Bissinger, S. M. Shafroth, and A. W. Waltner, Phys. Rev. A **5**, 246 (1972).

[2]P. Richard, T. I. Bonner, T. Furuta, I. L. Morgan, and J. R. Rhodes, Phys. Rev. A **1**, 1044 (1970).

[3]C. E. Busch, P. H. Nettles, W. K. Scates, S. M. Shafroth, and A. W. Waltner, Bull. Am. Phys. Soc. **17**, 500 (1972); Bull. Am. Phys. Soc. **17**, 499 (1972).

[4]G. Basbas, W. Brandt, and K. Laubert, Phys. Lett. A **34**, 277 (1971).

[5]E. Merzbacher and H. W. Lewis, in *Encyclopedia of Physics*, edited by S. Flugge (Springer-Verlag, Berlin, 1958), Vol. 34, p. 166.

[6]J. D. Garcia, Phys. Rev. A **1**, 280 (1970); Phys. Rev. A **1**, 1402 (1970).

[7]J. M. Hansteen and O. P. Mosebekk, Z. Phys. **234**, 281 (1970).

[8]G. A. Bissinger, A. B. Baskin, B.-H. Choi, S. M. Shafroth, J. M. Howard, and A. W. Waltner, Phys. Rev. A **6**, 545 (1972); S. M. Shafroth, G. A. Bissinger, and A. W. Waltner, Phys. Rev. A 7, 566 (1973).

[9]R. W. Fink, R. C. Jopson, Hans Mark, and C. D. Swift, Rev. Mod. Phys. **38**, 513 (1966).

[10]These PWBA calculations [B.-H. Choi (unpublished)] supersede the results of G. S. Khandelwal, B.-H. Choi, and E. Merzbacher [At. Data **1**, 103 (1969)].

[11]W. Bambynek, B. Crasemann, R. W. Fink, H.-U. Freund, H. Mark, C. D. Swift, R. E. Price, and P. W. Rao, Rev. Mod. Phys. **44**, 716 (1972).

[12]J. H. Scofield, Phys. Rev. **179**, 9 (1969).

PHYSICAL REVIEW A VOLUME 7, NUMBER 5 MAY 1973

Collision-Induced Absorption in Alkali-Metal-Atom–Inert-Gas Mixtures

C. Bottcher,* A. Dalgarno, and E. L. Wright

Harvard College Observatory and Smithsonian Astrophysical Observatory, Cambridge, Massachusetts 02138

(Received 10 October 1972)

Model potential calculations are presented of the ground-state potential curves and overlap dipole moments of the alkali-metal-atom–inert-gas-atom pairs LiHe, NaHe, LiNe, and NaNe. The coefficients of collision-induced absorption are evaluated for LiHe and NaHe at temperatures of 300 and 1000 °K using both quantum-mechanical and classical theories. The classical approximation accurately reproduces the quantum-mechanical results.

I. INTRODUCTION

In collision-induced absorption a photon is absorbed through the induced dipole moment of two unlike atoms:

$$(A+B)+h\nu \rightarrow (A+B)^* \ . \qquad (1)$$

The process may be regarded as inverse brems-